

See discussions, stats, and author profiles for this publication at: <https://www.researchgate.net/publication/261798361>

# Reactivities of Indenylruthenium Complex toward Internal Alkynes: Formation of Disubstituted Vinylidene Complexes and Indenyl–Alkyne Coupling

**DATASET** *in* ORGANOMETALLICS · JULY 2013

Impact Factor: 4.13 · DOI: 10.1021/om4004913

---

CITATIONS

6

---

READS

12

6 AUTHORS, INCLUDING:



**Yuichiro Mutoh**

Tokyo University of Science

46 PUBLICATIONS 519 CITATIONS

SEE PROFILE



**Youichi Ishii**

Chuo University

177 PUBLICATIONS 3,451 CITATIONS

SEE PROFILE

# Reactivities of Indenylruthenium Complex toward Internal Alkynes: Formation of Disubstituted Vinylidene Complexes and Indenyl–Alkyne Coupling

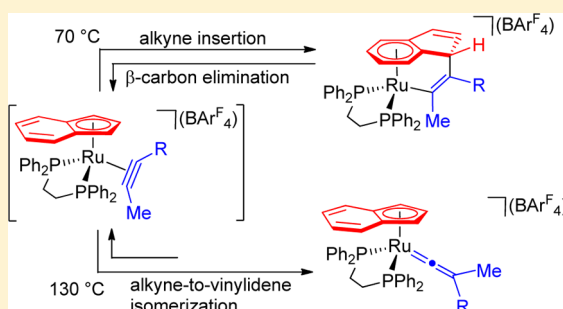
Yousuke Ikeda,<sup>†</sup> Yuichiro Mutoh,<sup>\*,†,§</sup> Kohei Imai,<sup>†</sup> Noriko Tsuchida,<sup>‡</sup> Keiko Takano,<sup>‡</sup> and Youichi Ishii<sup>\*,†</sup>

<sup>†</sup>Department of Applied Chemistry, Faculty of Science and Engineering, Chuo University, 1-13-27 Kasuga, Bunkyo-ku, Tokyo, 112-8551, Japan

<sup>‡</sup>Department of Chemistry and Biochemistry, Graduate School of Humanities and Sciences, Ochanomizu University, 2-1-1 Otsuka, Bunkyo-ku, Tokyo 112-8610, Japan

## S Supporting Information

**ABSTRACT:** Reaction of the indenylruthenium complex  $[(\eta^5\text{-C}_9\text{H}_7)\text{-RuCl}(\text{dppe})]$  with internal alkynes ( $\text{MeC}\equiv\text{CR}$ ,  $\text{R} = \text{Et}$ ,  $\text{Ph}$ ) in the presence of  $\text{NaBAR}^{\text{F}}_4$  gives rise to two types of C–C bond activation, i.e., alkyne insertion/ $\beta$ -carbon elimination and internal alkyne/disubstituted vinylidene rearrangement, as reversible processes. At 70 °C, regioisomeric complexes  $[\text{Ru}\{\text{C}(\text{Me})=\text{C}(\text{R})-(\eta^6\text{-C}_9\text{H}_7)\}(\text{dppe})][\text{BAR}^{\text{F}}_4]$  (**2**) and  $[\text{Ru}\{\text{C}(\text{R})=\text{C}(\text{Me})-(\eta^6\text{-C}_9\text{H}_7)\}(\text{dppe})][\text{BAR}^{\text{F}}_4]$  (**2'**) are formed through insertion of the alkyne into the Ru–indenyl bond followed by haptotropic rearrangement. Complexes **2'** isomerize completely to **2** at this temperature after longer reaction time. At 130 °C, **2** are further converted into the disubstituted vinylidene complexes  $[(\eta^5\text{-C}_9\text{H}_7)\text{Ru}\{\text{C}=\text{C}(\text{R})\text{Me}\}(\text{dppe})][\text{BAR}^{\text{F}}_4]$  (**3**) through alkyne–vinylidene rearrangement of the  $\eta^2$ -alkyne intermediate. This provides a rare example of direct observation of the  $\beta$ -carbon elimination from an unstrained transition metal alkenyl complex.



## INTRODUCTION

Vinylidene rearrangement of terminal alkynes at transition metal complexes as well as its applications for organic synthesis have been studied for more than 30 years, and its mechanistic details have been well documented in the literature.<sup>1</sup> On the other hand, formation of disubstituted vinylidene complexes from internal alkynes has not been recognized as a common process so far,<sup>1b,l</sup> although rearrangement of a few acyl alkynes to the corresponding vinylidenes has been reported.<sup>2</sup> We have recently demonstrated that even dialkyl- or diarylalkynes can take part in the potentially reversible vinylidene rearrangement at anionic and cationic iron and ruthenium complexes such as  $[\text{Ru}(\text{P}_3\text{O}_9)(\text{dppe})]^-$  ( $\text{dppe} = \text{Ph}_2\text{PCH}_2\text{CH}_2\text{PPh}_2$ ) and  $[\text{CpM}(\text{PP})]^+$  ( $\text{Cp} = \eta^5\text{-C}_5\text{H}_5$ ;  $\text{M} = \text{Ru}$ ,  $\text{Fe}$ ;  $\text{PP} = \text{dppe}$ ,  $2\text{PPh}_3$ ).<sup>3</sup> In this rearrangement, a more electron-withdrawing group shows higher migratory aptitude, and this tendency is opposite to that observed in common organic nucleophilic rearrangements. Interestingly, a DFT study has clarified that the rearrangement is nucleophilic in nature and accelerated by stabilization of a partial positive charge on the acceptor ( $\beta$ ) carbon in the transition state by the more electron-donating substituent.<sup>3e</sup>

To establish this rearrangement as a reliable and powerful activation method of internal alkynes, we have now paid attention to an indenylruthenium complex  $[(\eta^5\text{-C}_9\text{H}_7)\text{Ru}(\text{dppe})]^+$ , which can be conveniently generated from readily available  $[(\eta^5\text{-C}_9\text{H}_7)\text{RuCl}(\text{dppe})]$  (**1**),<sup>4</sup> as the reaction site. The

indenyl ligand is a better  $\pi$  acceptor in comparison with Cp and readily undergoes hapticity change.<sup>5</sup> We have envisioned that, by considering such effects, either the  $\eta^2$ -alkyne or  $\eta^1$ -disubstituted vinylidene complex can selectively be generated by adopting appropriate conditions. Quite unexpectedly, it has been found that the insertion of an internal alkyne into the Ru–indenyl bond and its back reaction, i.e.,  $\beta$ -carbon elimination, compete with the vinylidene rearrangement of the alkyne. These two types of C–C bond forming and cleaving reactions have been observed by varying the reaction temperature. The  $\beta$ -carbon elimination of transition metal alkyl complexes has been proposed as a key step in many transition-metal-catalyzed reactions.<sup>6</sup> Although this elementary process has been observed directly in several systems,<sup>7</sup> its reversibility has been exemplified only with strained ruthenacyclobutanes.<sup>7b,d</sup>

## RESULTS AND DISCUSSION

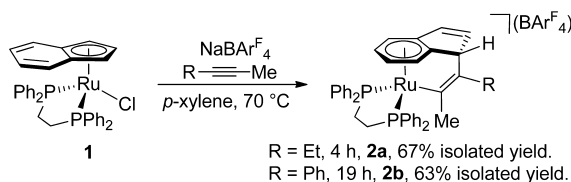
**Formation and Isomerization of Indenyl–Alkyne Coupling Complexes.** When complex **1** was allowed to react with  $\text{EtC}\equiv\text{CMe}$  (5 equiv) in the presence of  $\text{NaBAR}^{\text{F}}_4$  (1.2 equiv;  $\text{Ar}^{\text{F}} = 3,5\text{-(CF}_3)_2\text{C}_6\text{H}_3$ ) at 70 °C for 4 h in *p*-xylene, the  $^{31}\text{P}\{^1\text{H}\}$  NMR spectrum of the resulting yellow reaction

Received: May 30, 2013

Published: July 19, 2013

mixture revealed clear formation of a new complex, which showed a set of doublet resonances at  $\delta$  76.0 (d,  $^2J_{\text{PP}} = 35$  Hz) and  $\delta$  85.8 (d,  $^2J_{\text{PP}} = 35$  Hz), indicating the nonequivalence of the phosphorus nuclei of the product. Recrystallization of this yellow solution afforded the cyclometalated ( $\eta^6$ -indene) ruthenium complex  $[\text{Ru}\{\text{C}(\text{Me})=\text{C}(\text{Et})-(\eta^6\text{-C}_9\text{H}_7)\}(\text{dppe})][\text{BAR}^{\text{F}}_4]$  (**2a**), which is formed through indenyl–alkyne coupling in 67%, instead of the expected disubstituted vinylidene complex  $[(\eta^5\text{-C}_9\text{H}_7)\text{Ru}(\text{C}=\text{C}(\text{Et})\text{Me})(\text{dppe})][\text{BAR}^{\text{F}}_4]$  (**3a**) (Scheme 1). The  $^1\text{H}$  and  $^{13}\text{C}\{^1\text{H}\}$  NMR spectra

**Scheme 1.** Reaction of **1** with Internal Alkynes and  $\text{NaBAR}^{\text{F}}_4$



are in agreement with the proposed structure; the  $^{13}\text{C}$  resonance at  $\delta$  153.1 (t,  $^2J_{\text{CP}} = ^2J_{\text{CP}'} = 13$  Hz) assignable to the metal-bound alkenyl carbon of  $\text{Ru}-\text{C}(\text{Me})=\text{C}(\text{Et})$  is diagnostic of the indenyl–alkyne coupling product.

Finally, the molecular structure of **2a** has been determined unambiguously by a single-crystal X-ray diffraction study (Figure 1). Formation of the C2–C6 bond clearly indicates

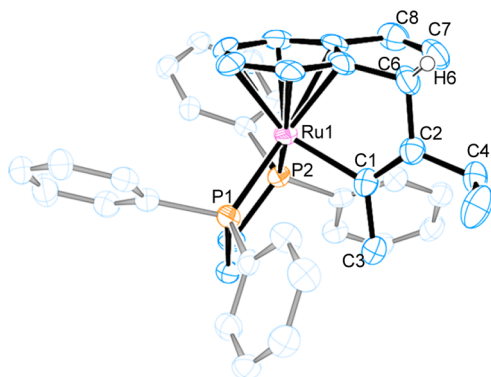


**Figure 1.** ORTEP drawing of **2a** (50% probability). Anionic part and hydrogen atoms except for H6 are omitted for clarity. Selected bond lengths (Å) and angles (deg): Ru1–C1, 2.116(5); C1–C2, 1.341(7); C1–C3, 1.527(7); C2–C4, 1.517(8); C2–C6, 1.523(8); C7–C8, 1.341(9); Ru1–C1–C2, 117.1(4); Ru1–C1–C3, 123.5(4); C2–C1–C3, 119.3(5); C1–C2–C4, 125.8(5); C1–C2–C6, 120.7(5); C4–C2–C6, 113.5(5).

the insertion of the alkyne into the Ru–indenyl bond with a syn stereochemistry, and at the same time the coordination mode of the indenyl moiety is slipped from  $\eta^5$  to  $\eta^6$ .<sup>5</sup> Complex **2a** adopts a typical three-legged piano–stool structure with the functionalized  $\eta^6$ -indene ligand, the two phosphorus atoms of dppe, and the alkenyl carbon atom. The Ru1–C1 bond length at 2.116(5) Å is consistent with a ruthenium–carbon single bond. The C1–C2 bond length (1.341(7) Å) as well as the planar geometry of these carbon atoms are also in good agreement with the formulation.

Similarly,  $[\text{Ru}\{\text{C}(\text{Me})=\text{C}(\text{Ph})-(\eta^6\text{-C}_9\text{H}_7)\}(\text{dppe})][\text{BAR}^{\text{F}}_4]$  (**2b**) was obtained from the reaction of **1**,  $\text{PhC}\equiv\text{CMe}$ , and  $\text{NaBAR}^{\text{F}}_4$  at 70 °C for 19 h. Although the later reaction provided a mixture of **2b** and the corresponding vinylidene complex  $[(\eta^5\text{-C}_9\text{H}_7)\text{Ru}(\text{C}=\text{C}(\text{Ph})\text{Me})(\text{dppe})][\text{BAR}^{\text{F}}_4]$  (**3b**) (vide infra)

**2b** could be isolated by simple recrystallization in 63% yield as yellow crystals (for the molecular structure of **2b**, see Supporting Information).

To gain deeper insight into the early stage of this reaction, we monitored the progress of the reaction of **1** with  $\text{EtC}\equiv\text{CMe}$  at 70 °C by means of  $^{31}\text{P}\{^1\text{H}\}$  NMR (Scheme 2, Figure

**Scheme 2.** Isomerization of **2'** to **2** at 70 °C

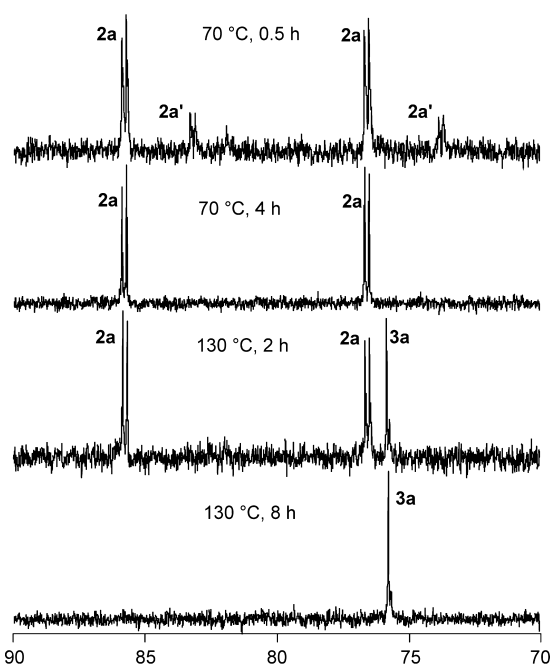
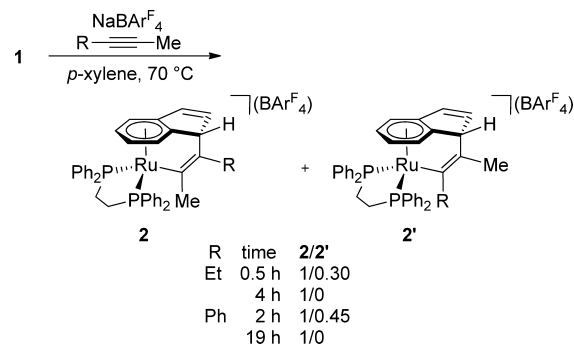


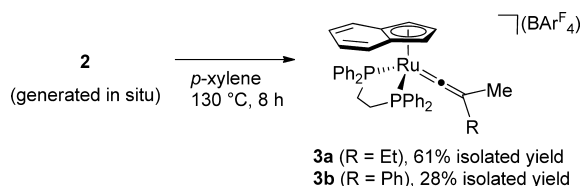
**Figure 2.**  $^{31}\text{P}\{^1\text{H}\}$  NMR spectra of the isomerization of **2a'** to **2a** at 70 °C, and **2a** to **3a** at 130 °C in *p*-xylene.

**2**). After 30 min, **1** was consumed completely, and two pairs of doublet signals were observed in the intensity ratio of 1:0.30. The major doublet is assigned to **2a**, whereas the minor one is attributable to the regioisomer of **2a**,  $[\text{Ru}\{\text{C}(\text{Et})=\text{C}(\text{Me})-(\eta^6\text{-C}_9\text{H}_7)\}(\text{dppe})][\text{BAR}^{\text{F}}_4]$  (**2a'**) on the basis of the  $^{31}\text{P}\{^1\text{H}\}$  NMR ( $\delta$  72.5 (d,  $^2J_{\text{PP}} = 35$  Hz) and 83.0 (d,  $^2J_{\text{PP}} = 35$  Hz)) and  $^{13}\text{C}\{^1\text{H}\}$  NMR ( $\delta$  158.5 (t,  $^2J_{\text{CP}} = ^2J_{\text{CP}'} = 13$  Hz)) data. One interesting feature of **2a'** is that it exhibits remarkably upfield shifted Et signals in the  $^1\text{H}$  NMR ( $\delta$  −0.29 (d,  $J = 7.4$  Hz, 3H,  $\text{CH}_2\text{CH}_3$ ), 0.91–0.64 (m, 2H,  $\text{CH}_2\text{CH}_3$ )), while the  $\text{CH}_3\text{—C}=\text{C}$  signal appears in the normal region ( $\delta$  1.77, s, 3H). This indicates the Et group is located close to one of the dppe Ph groups (vide infra).<sup>8</sup> On further heating, isomerization of **2a'** to

**2a** was observed, which completed in additional 3.5 h. A similar behavior was observed with  $\text{PhC}\equiv\text{CMe}$  albeit with a lower reaction rate; the reaction for 2 h at 70 °C gave a mixture of **2b** and  $[\text{Ru}\{\text{C}(\text{Ph})=\text{C}(\text{Me})-(\eta^6\text{-C}_9\text{H}_7)\}(\text{dppe})][\text{BAR}^{\text{F}}_4]$  (**2b'**) in the ratio of 1:0.45, and **2b'** was completely transformed into **2b** by heating for additional 17 h.

**Isomerization of 2 to Disubstituted Vinylidene Complexes 3.** A further reaction of **2** was observed at higher temperatures (Scheme 3). Thus, when a *p*-xylene solution of **2a**

Scheme 3. Isomerization of **2** to **3** at 130 °C



generated in situ was heated at 130 °C for 8 h,  $^{31}\text{P}\{^1\text{H}\}$  NMR spectra of the solution indicated complete transformation of **2a** into a new species, which exhibits one singlet at  $\delta$  75.8 (Figure 2). After recrystallization, the vinylidene complex  $[(\eta^5\text{-C}_9\text{H}_7)\text{-Ru}\{\text{C}=\text{C}(\text{Et})\text{Me}\}(\text{dppe})][\text{BAR}^{\text{F}}_4]$  (**3a**) was obtained in 61% yield as red crystals. Complex **3a** exhibits a  $^{13}\text{C}\{^1\text{H}\}$  NMR signal at  $\delta$  351.3 (t,  $^2J_{\text{CP}} = 17.0$  Hz) characteristic of the  $\alpha$  carbon of a vinylidene ligand, and its structure has been confirmed by X-ray analysis (Figure 3). The Ru1–C1 and C1–

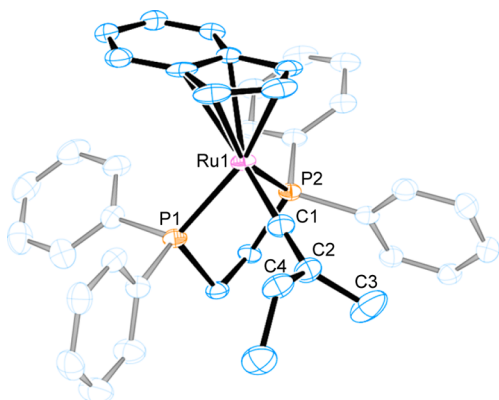


**Figure 3.** ORTEP drawing of **3a** (50% probability). Anionic part and hydrogen atoms are omitted for clarity. Selected bond lengths (Å) and angles (deg): Ru1–C1, 1.837(4); C1–C2, 1.315(5); Ru1–C1–C2, 174.0(3); C1–C2–C3, 125.3(4); C1–C2–C4, 118.7(3); C3–C2–C4, 115.9(3).

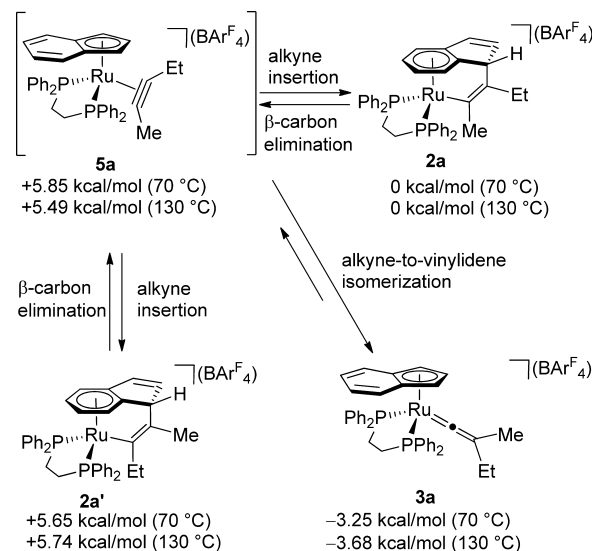
C2 bond distances of 1.837(4) Å and 1.315(5) Å, respectively, and the Ru1–C1–C2 bond angle of 174.0(3)° are comparable to those of known indenylruthenium vinylidene complexes.<sup>9</sup>

Although similar isomerization of **2b** to **3b**<sup>10</sup> was observed at 130 °C, the reaction for 8 h led to an equilibrium mixture of **2b** and **3b** in a ratio of 0.4:1 ( $^{31}\text{P}\{^1\text{H}\}$  NMR).<sup>11</sup> Fortunately, **3b** could be isolated by column chromatography on silica gel, albeit in low yield, and fully characterized by means of spectroscopic as well as crystallographic measurements (see Experimental Section). It is also interesting to note that the reaction of **1** with diphenylacetylene at 70 °C gives rise to the direct formation of diphenylvinylidene complex  $[(\eta^5\text{-C}_9\text{H}_7)\text{-Ru}(\text{C}=\text{CPh}_2)(\text{dppe})][\text{BAR}^{\text{F}}_4]$  (**4**) as the sole product, and the corresponding indenyl–alkyne coupling product was not

observed (for molecular structures of **3b** and **4**, see Supporting Information). We have previously reported that the diphenylacetylene exhibits relatively high reactivity toward the internal alkyne–disubstituted vinylidene rearrangement.<sup>3b</sup> In the present case, the vinylidene rearrangement of diphenylacetylene is considered to proceed faster than the indenyl–alkyne coupling (vide infra).

**Reaction Mechanisms.** Gimeno reported the formation of related  $\eta^6$ -indene complexes through the alkenyl–vinylidene complexes  $[(\eta^5\text{-C}_9\text{H}_7)\text{Ru}\{\text{C}=\text{C}(\text{H})\text{CR}^1\text{R}^2\text{CH}_2\text{CH}=\text{CH}_2\}(\text{PPh}_3)_2]^+$  ( $\text{R}^1, \text{R}^2 = \text{Ar}$ ).<sup>12</sup> Although its mechanism has not been clarified, intramolecular [2 + 2] cycloaddition<sup>13</sup> or direct carbocyclization<sup>14</sup> of the alkenyl–vinylidene ligand was suggested to be involved. However, we consider that the present reaction proceeds through a different process. Judging from the previous<sup>3a,b</sup> and above observations,  $\eta^2$ -alkyne complexes  $[(\eta^5\text{-C}_9\text{H}_7)\text{Ru}(\eta^2\text{-RC}\equiv\text{CMe})(\text{dppe})][\text{BAR}^{\text{F}}_4]$  (**5a**, R = Et; **5b**, R = Ph) should be involved as an intermediate (Scheme 4). Complex **2** and **2'** are competitively formed as the

Scheme 4. Gibbs Energy Differences of **2a'**, **3a**, and **5a** Relative to **2a**



kinetic products through insertion of an alkyne into the Ru–indenyl bond followed by haptotropic rearrangement of the indenyl ligand to an  $\eta^6$  fashion to form a stable 18e structure. On keeping at 70 °C, **2'** slowly isomerizes to **2** through the  $\beta$ -carbon elimination to regenerate the  $\eta^2$ -alkyne complex **5** followed by insertion of the alkyne into the Ru–indenyl bond with the opposite regiochemistry. Therefore **2a** and **2b** are the thermodynamic products at 70 °C. It should be pointed out that slippage of the ruthenium center from the  $\eta^6$ -arene structure in **2** (or **2'**) to the  $\eta^4$ -cyclopentadiene complex is a prerequisite for the  $\beta$ -carbon elimination. We consider that the coordinatively nonrigid nature of the indene and indenyl ligands should be an important factor for the present facile  $\beta$ -carbon elimination. At 130 °C, on the other hand, the alkyne-to-vinylidene isomerization of complex **5** starts to compete with the alkyne insertion, and the more thermodynamically favored **3** becomes the major product.<sup>15</sup>

The  $\beta$ -carbon elimination has recently been found to proceed with various transition metal complexes,<sup>6</sup> although that at ruthenium complexes is still uncommon.<sup>16</sup> In addition, to the



best of our knowledge, examples of  $\beta$ -carbon elimination at metal alkenyl complexes are very rare,<sup>7e,17</sup> and the reversible alkyne insertion/ $\beta$ -carbon elimination process in an unstrained system is unprecedented.<sup>7b,d</sup> Therefore, the present reaction provides the first example of competition of alkyne insertion/ $\beta$ -carbon elimination and alkyne/vinylidene rearrangement.

For better understanding of the above observation, preliminary density functional theory (DFT) calculations on the cationic part of **2a**, **2a'**, **3a**, and **5a** were performed with the M06 functional. The SDD effective core potential with the corresponding basis set on Ru and the 6-31G(d) basis set on the other atoms were employed for the Ru complexes. Gibbs free energies of **2a'**, **3a**, and **5a** relative to **2a** are listed in Scheme 4. Complex **2a'** and **5a** are comparable in energy at 70 °C, while **2a** is more stable in energy than **2a'** and **5a** by 5.65 and 5.85 kcal/mol, respectively. The higher stability of **2a** than **2a'** is attributable to the steric congestion between the Et substituent and one of the Ph groups of the dppe ligand. In fact, the CH<sub>3</sub> protons of the Et group exhibit remarkable upfield shift in the <sup>1</sup>H NMR (vide supra). Complex **3a** is the most stable among **2a**–**5a** at both 70 and 130 °C, and the energy difference between **2a** and **3a** is enlarged from 3.25 to 3.68 kcal/mol with increased temperature. These theoretical results could give good explanation for the relationship between the experimental findings and the relative Gibbs free energies of the products, although we have to await detailed DFT analysis to reveal structures and relative energies of transition states for these reactions.

## CONCLUSION

We have revealed that both internal alkyne/disubstituted vinylidene rearrangement and alkyne insertion/ $\beta$ -carbon elimination take place at an indenylruthenium complex as reversible processes. This reaction provides a rare example of direct observation of the  $\beta$ -carbon elimination from an unstrained transition metal alkenyl complex. Detailed mechanisms as well as the scope of these reactions are now under investigation.

## EXPERIMENTAL SECTION

**General Considerations.** All manipulations were carried out under an argon atmosphere by using standard Schlenk techniques unless otherwise stated. *p*-Xylene was dried over activated molecular sieves 4A, degassed by freeze–pump–thaw cycles, and stored under an argon atmosphere. The other solvents (dehydrated-grade) were purchased from Sigma-Aldrich and purged with argon before use. [ $(\eta^5\text{-C}_9\text{H}_7)\text{RuCl}(\text{dppe})$ ] (**1**),<sup>4</sup> and NaBARF<sub>4</sub>·2H<sub>2</sub>O<sup>18</sup> were synthesized according to the literature. <sup>1</sup>H (500 MHz), <sup>13</sup>C{<sup>1</sup>H} (126 MHz), and <sup>31</sup>P{<sup>1</sup>H} (202 MHz) NMR spectra were recorded on a JEOL ECA-500 spectrometer. Chemical shifts are reported in  $\delta$ , referenced to residual <sup>1</sup>H and <sup>13</sup>C signals of deuterated solvents as internal standards or to the <sup>31</sup>P signal of PPh<sub>3</sub> ( $\delta$  –5.65) as an external standard. IR spectra were recorded on a JASCO FT/IR-4200 spectrometer by using KBr pellets. Elemental analyses were performed on a Perkin-Elmer 2400 series II CHN analyzer. Amounts of the solvent molecules in the crystals were determined not only by elemental analyses but also by <sup>1</sup>H NMR spectroscopy.

**[Ru{C(Me)=C(Et)–( $\eta^6\text{-C}_9\text{H}_7$ )}](dppe)][BARF<sub>4</sub>] (**2a**).** A mixture of [ $(\eta^5\text{-C}_9\text{H}_7)\text{RuCl}(\text{dppe})$ ] (**1**; 26.2 mg, 0.040 mmol), NaBARF<sub>4</sub>·2H<sub>2</sub>O (48.0 mg, 0.052 mmol), and 2-pentyne (19  $\mu\text{L}$ , 0.20 mmol, 5 equiv) in *p*-xylene (2 mL) was stirred at 70 °C for 4 h. The resulting yellow suspension was filtered through a plug of Celite, and the plug was rinsed off with Et<sub>2</sub>O. The combined filtrate was dried in vacuo, and the residue was recrystallized from Et<sub>2</sub>O/hexanes to give **2a** (42.0 mg, 0.027 mmol, 67% yield) as yellow crystals. <sup>31</sup>P{<sup>1</sup>H} NMR (CD<sub>2</sub>Cl<sub>2</sub>):  $\delta$

85.8 (d, <sup>2</sup>J<sub>PP</sub> = 35 Hz, dppe), 76.0 (d, <sup>2</sup>J<sub>PP</sub> = 35 Hz, dppe). <sup>1</sup>H NMR (CD<sub>2</sub>Cl<sub>2</sub>):  $\delta$  7.88–7.00 (m, 32H, Ar), 6.71–6.61 (m, 2H, indenyl), 5.99–5.97 (m, 1H, indenyl), 5.16–5.14 (m, 1H, indenyl), 4.64–4.57 (m, 2H, indenyl), 4.36 (br, 1H, indenyl), 3.13–2.69 (m, 4H, CH<sub>2</sub> of dppe), 2.14–1.93 (m, 2H, CH<sub>2</sub>CH<sub>3</sub>), 1.03 (t, 3H, CH<sub>2</sub>CH<sub>3</sub>), 0.53 (s, 3H, CH<sub>3</sub>). Selected <sup>13</sup>C{<sup>1</sup>H} NMR (CD<sub>2</sub>Cl<sub>2</sub>):  $\delta$  154.2 (s, Ru–C≡C), 153.1 (t, <sup>2</sup>J<sub>CP</sub> = <sup>2</sup>J<sub>CP</sub> = 13 Hz, Ru–C(Me)), 121.2 (s, indenyl), 109.5 (d, *J* = 8.1 Hz, indenyl), 101.9 (d, *J* = 4.0 Hz, indenyl), 99.7 (d, *J* = 4.0 Hz, indenyl), 87.5 (s, indenyl), 79.5 (d, *J* = 10.1 Hz, indenyl), 59.6 (s, indenyl), 29.6 (dd, *J* = 6.0, 13.1 Hz, CH<sub>2</sub> of dppe), 29.4 (m, CH<sub>2</sub> of dppe and CH<sub>3</sub>), 27.4 (s, CH<sub>2</sub>CH<sub>3</sub>), 12.9 (s, CH<sub>2</sub>CH<sub>3</sub>). Many of the Ph signals are overlapping and could not be assigned. Anal. Calcd for C<sub>72</sub>H<sub>51</sub>BF<sub>4</sub>P<sub>2</sub>Ru (**2a**): C, 55.94; H, 3.33. Found: C, 56.06; H, 3.16.

**[Ru{C(Me)=C(Ph)–( $\eta^6\text{-C}_9\text{H}_7$ )}](dppe)][BARF<sub>4</sub>] (**2b**).** A mixture of [ $(\eta^5\text{-C}_9\text{H}_7)\text{RuCl}(\text{dppe})$ ] (**1**; 24.7 mg, 0.038 mmol), NaBARF<sub>4</sub>·2H<sub>2</sub>O (42.6 mg, 0.046 mmol), and 1-phenyl-1-propyne (24  $\mu\text{L}$ , 0.194 mmol, 5 equiv) in *p*-xylene (2 mL) was stirred at 70 °C for 19 h. The <sup>31</sup>P{<sup>1</sup>H} NMR spectrum of the reaction mixture indicated complete consumption of **1** and formation of **2b** ( $\delta$  86.4 and 77.8) and **3b** ( $\delta$  75.1) in a ratio of 1/0.05. The resulting yellow solution was filtered through a plug of Celite, and the plug was rinsed off with Et<sub>2</sub>O. The combined filtrate was dried in vacuo, and the residue was recrystallized from Et<sub>2</sub>O–benzene/hexane. Two kinds of crystals, i.e., the yellow blocks (**2b**) and red microcrystals (**3b**) were deposited as a mixture. The yellow blocks were separated manually from the mixture and recrystallized from Et<sub>2</sub>O/hexane to afford **2b**·0.5Et<sub>2</sub>O (39.0 mg, 0.024 mmol, 63% yield). Single crystals of **2b**·C<sub>6</sub>H<sub>6</sub> suitable for X-ray analysis were obtained by recrystallization from benzene/hexane. <sup>31</sup>P{<sup>1</sup>H} NMR (CD<sub>2</sub>Cl<sub>2</sub>):  $\delta$  86.6 (d, <sup>2</sup>J<sub>PP</sub> = 35 Hz, dppe), 77.9 (d, <sup>2</sup>J<sub>PP</sub> = 35 Hz, dppe). <sup>1</sup>H NMR (CD<sub>2</sub>Cl<sub>2</sub>):  $\delta$  7.97–7.04 (m, 37H, Ar), 6.84–6.83 (m, 1H, indenyl), 6.66–6.65 (m, 1H, indenyl), 6.20–6.19 (m, 1H, indenyl), 5.36–5.34 (m, 1H, indenyl), 4.68–4.64 (m, 2H, indenyl), 4.57 (br, 1H, indenyl), 3.15–2.75 (m, 4H, CH<sub>2</sub> of dppe), 0.47 (s, 3H, CH<sub>3</sub>). Selected <sup>13</sup>C{<sup>1</sup>H} NMR (CD<sub>2</sub>Cl<sub>2</sub>):  $\delta$  158.2 (t, <sup>2</sup>J<sub>CP</sub> = <sup>2</sup>J<sub>CP</sub> = 13 Hz, Ru–C–Me), 153.4 (s, Ru–C≡C), 121.1 (s, indenyl), 110.3 (d, *J* = 8.1 Hz, indenyl), 102.7 (d, *J* = 3.0 Hz, indenyl), 99.5 (d, *J* = 3.0 Hz, indenyl), 87.9 (s, indenyl), 79.7 (d, *J* = 9.1 Hz, indenyl), 61.7 (s, indenyl), 31.0 (dd, *J* = 3.6, 6.0 Hz, CH<sub>3</sub>), 29.9 (m, CH<sub>2</sub> of dppe). Many of the Ph signals are overlapping and could not be assigned. Anal. Calcd for C<sub>78</sub>H<sub>56</sub>BF<sub>4</sub>O<sub>0.5</sub>P<sub>2</sub>Ru (**2b**·0.5Et<sub>2</sub>O): C, 57.44; H, 3.46. Found: C, 57.70; H, 3.28.

**[ $(\eta^5\text{-C}_9\text{H}_7)\text{Ru}(\text{C}(\text{Me})=\text{C}(\text{Et})\text{Me})(\text{dppe})$ ][BARF<sub>4</sub>] (**3a**).** A mixture of [ $(\eta^5\text{-C}_9\text{H}_7)\text{RuCl}(\text{dppe})$ ] (**1**; 27.2 mg, 0.042 mmol), NaBARF<sub>4</sub>·2H<sub>2</sub>O (43.0 mg, 0.047 mmol), and 2-pentyne (19  $\mu\text{L}$ , 0.206 mmol, 5 equiv) in *p*-xylene (2 mL) was stirred at 70 °C for 4 h. The <sup>31</sup>P{<sup>1</sup>H} NMR of the reaction mixture indicated the formation of **2a** as the sole product. Then, the resulting yellow suspension was heated at 130 °C for 8 h. The orange reaction mixture was filtered through a plug of Celite, and the plug was rinsed with Et<sub>2</sub>O. The combined filtrate was dried in vacuo, and the residue was recrystallized from Et<sub>2</sub>O/hexanes to give **3a** (39.4 mg, 0.026 mmol, 61% yield) as red crystals. <sup>31</sup>P{<sup>1</sup>H} NMR (CD<sub>2</sub>Cl<sub>2</sub>):  $\delta$  76.0 (s, dppe). <sup>1</sup>H NMR (CD<sub>2</sub>Cl<sub>2</sub>):  $\delta$  7.71–6.86 (m, 36H, Ar), 5.72 (br, 2H, indenyl), 5.67 (br, 1H, indenyl), 2.61–2.40 (m, 4H, CH<sub>2</sub> of dppe), 1.09 (q, *J* = 7.4 Hz, 2H, CH<sub>2</sub>CH<sub>3</sub>), 0.82 (s, 3H, Me), 0.55 (t, *J* = 7.4 Hz, 3H, CH<sub>2</sub>CH<sub>3</sub>). Selected <sup>13</sup>C{<sup>1</sup>H} NMR (CD<sub>2</sub>Cl<sub>2</sub>):  $\delta$  351.3 (t, <sup>2</sup>J<sub>CP</sub> = 17.0 Hz, Ru=C=C), 121.8 (s, Ru=C=C), 96.3 (s, indenyl), 78.2 (s, indenyl), 27.2 (pseudo t, *J* = 24.2 Hz, CH<sub>2</sub> of dppe), 18.3 (s, CH<sub>2</sub>CH<sub>3</sub>), 13.7 (s, CH<sub>2</sub>CH<sub>3</sub>), 7.06 (s, CH<sub>3</sub>). Many of the Ph signals are overlapping and could not be assigned. IR (cm<sup>–1</sup>): 1682 (m,  $\nu_{\text{C}=\text{C}}$ ). Anal. Calcd for C<sub>72</sub>H<sub>51</sub>BF<sub>4</sub>P<sub>2</sub>Ru (**3a**): C, 55.94; H, 3.33. Found: C, 55.74; H, 3.10.

**[ $(\eta^5\text{-C}_9\text{H}_7)\text{Ru}(\text{C}(\text{Me})=\text{C}(\text{Ph})\text{Me})(\text{dppe})$ ][BARF<sub>4</sub>] (**3b**).** A mixture of [ $(\eta^5\text{-C}_9\text{H}_7)\text{RuCl}(\text{dppe})$ ] (**1**; 30.3 mg, 0.047 mmol), NaBARF<sub>4</sub>·2H<sub>2</sub>O (51.9 mg, 0.056 mmol), and 1-phenyl-1-propyne (30  $\mu\text{L}$ , 0.243 mmol, 5 equiv) in *p*-xylene (3 mL) was stirred at 70 °C for 19 h. After the formation of a mixture of **2b** and **3b** was confirmed by <sup>31</sup>P{<sup>1</sup>H} NMR, the resulting yellow suspension was heated at 130 °C for 8 h. The <sup>31</sup>P NMR spectrum of the orange reaction mixture indicated the formation of **3b** ( $\delta$  75.1) and **2b** ( $\delta$  86.4 and 77.8) in a ratio of 1/0.4. The

mixture was filtered through a plug of Celite, and the plug was rinsed off with Et<sub>2</sub>O. The combined filtrate was dried under a vacuum, and the residue was chromatographed on silica gel (eluent CH<sub>2</sub>Cl<sub>2</sub>/Et<sub>2</sub>O = 1/4). The orange fraction was collected and dried under a vacuum, and the residue was recrystallized from Et<sub>2</sub>O/hexane to afford **3b** (21.4 mg, 0.013 mmol, 28% yield) as red crystals. <sup>31</sup>P{<sup>1</sup>H} NMR (CD<sub>2</sub>Cl<sub>2</sub>): δ 75.1 (s, dppe). <sup>1</sup>H NMR (CD<sub>2</sub>Cl<sub>2</sub>): δ 7.73–6.49 (m, 41H, Ar), 5.89 (br, 1H, indenyl), 5.86 (br, 2H, indenyl), 2.72–2.66 (m, 2H, CH<sub>2</sub> of dppe), 2.58–2.52 (m, 2H, CH<sub>2</sub> of dppe), 1.21 (s, 3H, Me). Selected <sup>13</sup>C{<sup>1</sup>H} NMR (CD<sub>2</sub>Cl<sub>2</sub>): δ 356.1 (t, <sup>2</sup>J<sub>CP</sub> = 17.2 Hz, Ru=C=C), 123.6 (s, Ru=C=C), 96.7 (s, indenyl), 79.2 (s, indenyl), 27.1 (pseudo t, J = 23.7 Hz, CH<sub>2</sub> of dppe), 8.73 (s, CH<sub>3</sub>). Many of the Ph signals are overlapping and could not be assigned. IR (KBr, cm<sup>-1</sup>): 1639 (m, ν<sub>C=C</sub>). Anal. Calcd for C<sub>76</sub>H<sub>51</sub>BF<sub>24</sub>P<sub>2</sub>Ru (**3b**): C, 57.27; H, 3.22. Found: C, 57.11; H, 3.06.

[(η<sup>5</sup>-C<sub>9</sub>H<sub>7</sub>)Ru(=C=CPh<sub>2</sub>)(dppe)][BAR<sub>4</sub><sup>F</sup>] (**4**). A mixture of [(η<sup>5</sup>-C<sub>9</sub>H<sub>7</sub>)RuCl(dppe)] (**1**; 29.3 mg, 0.045 mmol), NaBAR<sub>4</sub><sup>F</sup>·2H<sub>2</sub>O (50.9 mg, 0.055 mmol), and diphenylacetylene (40.2 mg, 0.226 mmol, 5 equiv) in *p*-xylene (2 mL) was stirred at 70 °C for 1 h. The resulting red suspension was filtered through a plug of Celite, and the plug was rinsed off with Et<sub>2</sub>O. The combined filtrate was dried in vacuo, and the residue was recrystallized from Et<sub>2</sub>O/hexanes to give **4** (56.6 mg, 0.034 mmol, 76% yield) as red crystals. <sup>31</sup>P{<sup>1</sup>H} NMR (CD<sub>2</sub>Cl<sub>2</sub>): δ 75.2 (s, dppe). <sup>1</sup>H NMR (CD<sub>2</sub>Cl<sub>2</sub>): δ 7.75–6.50 (m, 46H, Ar), 5.99–5.95 (m, 3H, indenyl), 3.04–2.92 (m, 2H, CH<sub>2</sub> of dppe), 2.73–2.61 (m, 2H, CH<sub>2</sub> of dppe). Selected <sup>13</sup>C{<sup>1</sup>H} NMR (CD<sub>2</sub>Cl<sub>2</sub>): δ 351.1 (t, <sup>2</sup>J<sub>CP</sub> = 16.7 Hz, Ru=C=C), 133.1 (s, Ru=C=C), 97.6 (s, indenyl), 80.2 (s, indenyl), 27.2 (pseudo t, J = 23.7 Hz, CH<sub>2</sub> of dppe). Many of the Ph signals are overlapping and could not be assigned. IR (cm<sup>-1</sup>): 1626 (w, ν<sub>C=C</sub>). Anal. Calcd for C<sub>81</sub>H<sub>53</sub>BF<sub>24</sub>P<sub>2</sub>Ru (**4**): C, 58.75; H, 3.23. Found: C, 58.36; H, 3.07.

**X-ray Diffraction Studies.** Diffraction data for **2a**, **2b**·C<sub>6</sub>H<sub>6</sub>, **3a**, **3b**, and **4** were collected on a Rigaku Mercury CCD area detector with graphite-monochromated Mo Kα radiation (λ = 0.71070 Å) at -150 °C. Intensity data were corrected for Lorenz-polarization effects and for empirical absorption (REQAB).<sup>19</sup> All calculations were performed using the *CrystalStructure*<sup>20</sup> crystallographic software package except for refinements, which were performed using SHELXL-97.<sup>21</sup> The positions of the non-hydrogen atoms were determined by direct methods (SIR-2008<sup>22</sup>) and subsequent Fourier syntheses (DIRDIF-99).<sup>23</sup> All non-hydrogen atoms were refined on F<sub>o</sub><sup>2</sup> anisotropically by full-matrix least-squares techniques. All hydrogen atoms were placed at the calculated positions with fixed isotropic parameters. Details of the X-ray diffraction study are summarized in Table S1 and S2 (Supporting Information). Molecular structures of **2b**, **3b**, and **4** with selected bond lengths and angles are shown in Figures S1, S2, and S3 (Supporting Information). Although there are some alerts of type B due to the disorder of some of the CF<sub>3</sub> groups in the BAR<sub>4</sub><sup>F</sup> anions, they do not affect the results of the structural determination.

**Computational Details.** All density functional theory (DFT) calculations were performed using the Gaussian 09 package.<sup>24</sup> The computers used in the present study are Linux PC cluster machines at Ochanomizu University and the computer facilities at the Research Center for Computational Science in Okazaki, Japan. Geometries of the cationic part of **2a**, **2a'**, **3a**, and **5a** were fully optimized using the M06<sup>25</sup> density functional with the effective core potential (ECP) and basis sets: the Stuttgart/Dresden (SDD) ECP with the corresponding basis set for Ru<sup>26,27</sup> and the 6-31G(d)\* basis set for the remaining nonmetal atoms. The combined basis set is denoted as SDD-6-31G(d) throughout this article. Vibrational analysis based on the force constant matrices (Hessians) was carried out at the stationary points in order to identify them as minima (all positive constants), transition states (one negative force constant), or higher-order saddle points. Optimized Cartesian coordinates were summarized in Tables S3–S6 (Supporting Information). The optimized structures of the cationic part of **2a** and **3a** in the ground state along with the selected calculated structural parameters and the experimental values obtained by X-ray crystallography are summarized in Tables S7 and S9 (Supporting Information). The local minimum structures of complexes **2a'** and **5a** with the selected structural parameters are summarized in Tables S8

and S10 (Supporting Information). The potential energy differences relative to **2a** are described in the main text of this paper.

## ■ ASSOCIATED CONTENT

### Supporting Information

Text, figures, and CIF files giving details of DFT calculations and crystallographic data. This material is available free of charge via the Internet at <http://pubs.acs.org>.

## ■ AUTHOR INFORMATION

### Corresponding Author

\*E-mail: [ymutoh@rs.tus.ac.jp](mailto:ymutoh@rs.tus.ac.jp) (Y.M.); [yo-ishii@kc.chuo-u.ac.jp](mailto:yo-ishii@kc.chuo-u.ac.jp) (Y.I.).

### Present Address

<sup>§</sup>Department of Chemistry, Faculty of Science, Tokyo University of Science, 1-3 Kagurazaka, Shinjuku-ku, Tokyo 162-8601, Japan.

### Notes

The authors declare no competing financial interest.

## ■ ACKNOWLEDGMENTS

We thank the Research Center for Computational Science in Okazaki, Japan, for the use of the computer facilities. This research was supported by a Grant-in-Aid for Scientific Research on Innovative Areas “Molecular Activation Directed toward Straightforward Synthesis” (23105543) from the MEXT of Japan.

## ■ REFERENCES

- (1) For reviews, see: (a) *Metal Vinylidenes and Allenylidenes in Catalysis: From Reactivity to Applications in Synthesis*; Bruneau, C., Dixneuf, P. H., Eds.; Wiley-VCH: Weinheim, Germany, 2008. (b) Marinelli, G.; Streib, W. E.; Huffma, J. C.; Caulton, K. G.; Gagné, M. R.; Takats, J.; Dartiguenave, M.; Chardon, C.; Jackson, S. A.; Eisenstein, O. *Polyhedron* **1990**, *9*, 1867–1881. (c) Bruce, M. I. *Chem. Rev.* **1991**, *91*, 197–257. (d) Bruneau, C.; Dixneuf, P. H. *Acc. Chem. Res.* **1999**, *32*, 311–323. (e) Valerga, P.; Puerta, M. C. *Coord. Chem. Rev.* **1999**, *193*–195, 977–1025. (f) Wakatsuki, Y. *J. Organomet. Chem.* **2004**, *689*, 4092–4109. (g) Cadierno, V.; Gamasa, M. P.; Gimeno, J. *Coord. Chem. Rev.* **2004**, *248*, 1627–1657. (h) Trost, B. M.; Frederiksen, M. U.; Rudd, M. T. *Angew. Chem., Int. Ed.* **2005**, *44*, 6630–6666. (i) Bruneau, C.; Dixneuf, P. H. *Angew. Chem., Int. Ed.* **2006**, *45*, 2176–2203. (j) Varela, J. A.; Saá, C. *Chem.—Eur. J.* **2006**, *12*, 6450–6456. (k) Trost, B. M.; McClory, A. *Chem.—Asian J.* **2008**, *3*, 164–194. (l) Lynam, J. M. *Chem.—Eur. J.* **2010**, *16*, 8238–8247.
- (2) (a) King, P. J.; Knox, S. A. R.; Legge, M. S.; Orpen, A. G.; Wilkinson, J. N.; Hill, E. A. *J. Chem. Soc., Dalton Trans.* **2000**, 1547–1548. (b) Shaw, M. J.; Bryant, S. W.; Rath, N. *Eur. J. Inorg. Chem.* **2007**, 3943–3946. (c) de los Rios, I.; Bustelo, E.; Puerta, M. C.; Valerga, P. *Organometallics* **2010**, *29*, 1740–1749. (d) Singh, V. K.; Bustelo, E.; de los Rios, I.; Macías-Arce, I.; Puerta, M. C.; Valerga, P.; Ortuño, M. A.; Ujaque, G.; Lledós, A. *Organometallics* **2011**, *30*, 4014–4031. (e) Fernández, F. E.; Puerta, M. C.; Valerga, P. *Inorg. Chem.* **2013**, *52*, 6502–6509.
- (3) (a) Ikeda, Y.; Yamaguchi, T.; Kanao, K.; Kimura, K.; Kamimura, S.; Mutoh, Y.; Tanabe, Y.; Ishii, Y. *J. Am. Chem. Soc.* **2008**, *130*, 16856–16857. (b) Mutoh, Y.; Ikeda, Y.; Kimura, Y.; Ishii, Y. *Chem. Lett.* **2009**, *38*, 534–535. (c) Mutoh, Y.; Imai, K.; Kimura, Y.; Ikeda, Y.; Ishii, Y. *Organometallics* **2011**, *30*, 204–207. (d) Mutoh, Y.; Kimura, Y.; Ikeda, Y.; Tsuchida, N.; Takano, K.; Ishii, Y. *Organometallics* **2012**, *31*, 5150–5158. (e) Otsuka, M.; Tsuchida, N.; Ikeda, Y.; Kimura, Y.; Mutoh, Y.; Ishii, Y.; Takano, K. *J. Am. Chem. Soc.* **2012**, *134*, 17746–17756.
- (4) Oro, L. A.; Ciriano, M. A.; Campo, M. J. *Organomet. Chem.* **1985**, *289*, 117–131.

- (5) (a) Hartwig, J. F. In *Organotransition Metal Chemistry: From Bonding to Catalysis*; University Science Books: Sausalito, CA, 2010; pp 250–253. (b) O'Connor, J. M.; Casey, C. P. *Chem. Rev.* **1987**, *87*, 307–318. (c) Calhorda, M. J.; Veiros, L. F. *Coord. Chem. Rev.* **1999**, *185–186*, 37–51. (d) Cadierno, V.; Díez, J.; Gamasa, M. P.; Gimeno, J.; Lastra, E. *Coord. Chem. Rev.* **1999**, *193–195*, 147–205. (e) Veiros, L. F. *Organometallics* **2000**, *19*, 3127–3136. (f) Zargarian, D. *Coord. Chem. Rev.* **2002**, *233–234*, 157–176. (g) Calhorda, M. J.; Romão, C. C.; Veiros, L. F. *Chem.—Eur. J.* **2002**, *8*, 868–875.
- (6) Recent example: (a) Murakami, M.; Makino, M.; Ashida, S.; Matsuda, T. *Bull. Chem. Soc. Jpn.* **2006**, *79*, 1315–1321. (b) Murakami, M.; Matsuda, T. *Chem. Commun.* **2011**, 1100–1105. (c) Seiser, T.; Saget, T.; Tran, D. N.; Cramer, N. *Angew. Chem., Int. Ed.* **2011**, *50*, 7740–7752. (d) Cramer, N.; Seiser, T. *Synlett* **2011**, 449–460. (e) Aissa, C. *Synthesis* **2011**, 3389–3407. (f) Ruhland, K. *Eur. J. Org. Chem.* **2012**, 2683–2706. (g) Bour, J. R.; Green, J. C.; Winton, V. J.; Johnson, J. B. *J. Org. Chem.* **2013**, *78*, 1665–1669.
- (7) (a) Hartwig, J. F.; Bergman, R. G.; Andersen, R. A. *Organometallics* **1991**, *10*, 3344–3362. (b) McNeill, K.; Andersen, R. A.; Bergman, R. G. *J. Am. Chem. Soc.* **1995**, *117*, 3625–3626. (c) Dimauro, P. T.; Wolczanski, P. T. *Polyhedron* **1995**, *14*, 149–165. (d) McNeill, K.; Andersen, R. A.; Bergman, R. G. *J. Am. Chem. Soc.* **1997**, *119*, 11244–11254. (e) Etienne, M.; Mathieu, R.; Donnadieu, B. *J. Am. Chem. Soc.* **1997**, *119*, 3218–3228. (f) Zhao, P.; Hartwig, J. F. *J. Am. Chem. Soc.* **2005**, *127*, 11618–11619. (g) Zao, P.; Incarvito, C. D.; Hartwig, J. F. *J. Am. Chem. Soc.* **2006**, *128*, 3124–3125. (h) Zhao, P.; Hartwig, J. F. *Organometallics* **2008**, *27*, 4749–4757.
- (8) For complex **2a**, the CH<sub>3</sub>–C protons resonate at an upfield shifted region ( $\delta$  0.53, s, 3H), suggesting that this CH<sub>3</sub> group is close to a Ph group of dppe.
- (9) (a) Gamasa, M. P.; Gimeno, J.; Martín-Vaca, B. M.; Borge, J.; García-Granda, S.; Pérez-Carreño, E. *Organometallics* **1994**, *13*, 4045–4057. (b) Cadierno, V.; Gamasa, M. P.; Gimeno, J.; Borge, J.; García-Granda, S. *Organometallics* **1997**, *16*, 3178–3187. (c) Sung, H. L.; Hsu, H. L. *J. Organomet. Chem.* **2011**, *696*, 1280–1288.
- (10) The triflate analogue complex  $[(\eta^5\text{-C}_9\text{H}_7)\text{Ru}\{\text{C}\equiv\text{CPh(Me)}\}\text{dppe}](\text{OTf})$  can be prepared by methylation of the alkynyl complex  $[(\eta^5\text{-C}_9\text{H}_7)\text{Ru}(\text{C}\equiv\text{CPh})(\text{dppe})]$  with methyl triflate; see ref 9a.
- (11) When isolated complex **3b** was heated at 130 °C for 8 h in *p*-xylene, a mixture of **2b** and **3b** was formed in a ratio of 0.4:1 (<sup>31</sup>P{<sup>1</sup>H} NMR).
- (12) Cadierno, V.; Conejero, S.; Díez, J.; Gamasa, M. P.; Gimeno, J.; García-Granda, S. *Chem. Commun.* **2003**, 840–841.
- (13) Álvarez, P.; Lastra, E.; Gimeno, J.; Bassetti, M.; Falvello, L. R. *J. Am. Chem. Soc.* **2003**, *125*, 2386–2387.
- (14) Merlic, C. A.; Pauly, M. E. *J. Am. Chem. Soc.* **1996**, *118*, 11319–11320.
- (15) Internal alkynes-to-disubstituted vinylidene rearrangement is potentially reversible reaction (see ref 3c).
- (16)  $\beta$ -Carbon elimination of ruthenium complex: ref 7a–d and (a) Kondo, T.; Kodoi, K.; Nishinaga, E.; Okada, T.; Morisaki, Y.; Watanabe, Y.; Mitsudo, T. *J. Am. Chem. Soc.* **1998**, *120*, 5587–5588. (b) Older, C. M.; Stryker, J. M. *J. Am. Chem. Soc.* **2000**, *122*, 2784–2797. (c) Sakaki, S.; Ohki, T.; Takayama, T.; Sugimoto, M.; Kondo, T.; Mitsudo, T. *Organometallics* **2001**, *20*, 3145–3158.
- (17)  $\beta$ -Carbon elimination reactions from iminyl complexes were reported by Uemura and Hartwig; see ref 7f, 7h, and (a) Nishimura, T.; Uemura, S. *J. Am. Chem. Soc.* **2000**, *122*, 12049–12050. (b) Nishimura, T.; Nishiguchi, Y.; Maeda, Y.; Uemura, S. *J. Org. Chem.* **2004**, *69*, 5342–5347.
- (18) (a) Reger, D. L.; Wright, T. D.; Little, C. A.; Lamba, J. J. S.; Smith, M. D. *Inorg. Chem.* **2001**, *40*, 3810–3814. (b) Reger, D. L.; Little, C. A.; Little, C. A.; Lamba, J. J. S.; Brown, K. J. *Inorg. Synth.* **2004**, *34*, 5–8. (c) Smith, C. R.; Zhang, A.; Mans, D. J.; BajanBabu, T. V. *Org. Synth.* **2008**, *85*, 248–266.
- (19) Jacobson, R. A. *Private Communication to Rigaku Corp.*; Rigaku Corp.: Tokyo, Japan, 1998.
- (20) *CrystalStructure 4.0: Single Crystal Structure Analysis Package*; Rigaku Corporation: Tokyo, Japan, 2000–2010.
- (21) Sheldrick, G. M. *Acta Crystallogr., Sect. A* **2008**, *64*, 112–122.
- (22) Burla, M. C.; Caliendo, R.; Camalli, M.; Carrozzini, B.; Cascarano, G. L.; De Caro, L.; Giacovazzo, C.; Polidori, G.; Siliqi, D.; Spagna, R. *J. Appl. Crystallogr.* **2007**, *40*, 609–613.
- (23) Beurskens, P. T.; Beurskens, G.; de Gelder, R.; García-Granda, S.; Gould, R. O.; Israël, R.; Smits, J. M. M. *The DIRDIF-99 Program System*; Crystallography Laboratory, University of Nijmegen: The Netherlands, 1999.
- (24) Frisch, M. J.; Trucks, G. W.; Schlegel, H. B.; Scuseria, G. E.; Robb, M. A.; Cheeseman, J. R.; Scalmani, G.; Barone, V.; Mennucci, B.; Petersson, G. A.; Nakatsuji, H.; Caricato, M.; Li, X.; Hratchian, H. P.; Izmaylov, A. F.; Bloino, J.; Zheng, G.; Sonnenberg, J. L.; Hada, M.; Ehara, M.; Toyota, K.; Fukuda, R.; Hasegawa, J.; Ishida, M.; Nakajima, T.; Honda, Y.; Kitao, O.; Nakai, H.; Vreven, T.; Montgomery, Jr., J. A.; Peralta, J. E.; Ogliaro, F.; Bearpark, M.; Heyd, J. J.; Brothers, E.; Kudin, K. N.; Staroverov, V. N.; Kobayashi, R.; Normand, J.; Raghavachari, K.; Rendell, A.; Burant, J. C.; Iyengar, S. S.; Tomasi, J.; Cossi, M.; Rega, N.; Millam, J. M.; Klene, M.; Knox, J. E.; Cross, J. B.; Bakken, V.; Adamo, C.; Jaramillo, J.; Gomperts, R.; Stratmann, R. E.; Yazyev, O.; Austin, A. J.; Cammi, R.; Pomelli, C.; Ochterski, J. W.; Martin, R. L.; Morokuma, K.; Zakrzewski, V. G.; Voth, G. A.; Salvador, P.; Dannenberg, J. J.; Dapprich, S.; Daniels, A. D.; Farkas, O.; Foresman, J. B.; Ortiz, J. V.; Cioslowski, J.; Fox, D. J. *Gaussian 09*, Revision A.02; Gaussian, Inc.: Wallingford, CT, 2009.
- (25) Zhao, Y.; Truhlar, D. G. *Theor. Chem. Acc.* **2008**, *120*, 215–241.
- (26) Dolg, M.; Wedig, U.; Stoll, H.; Preuss, H. *J. Chem. Phys.* **1987**, *86*, 866–872.
- (27) Andrae, D.; Häußermann, U.; Dolg, M.; Stoll, H.; Preuß, H. *Theor. Chim. Acta.* **1990**, *77*, 123–141.